Article

pubs.acs.org/Biomac

Macromolecular Hydrogen Sulfide Donors Trigger Spatiotemporally Confined Changes in Cell Signaling

Francesca Ercole,[†] Friederike M. Mansfeld,[†,‡] Maria Kavallaris,[‡,§] Michael R. Whittaker,[†] John F. Quinn,*[,†] Michelle L. Halls,*[,∥] and Thomas P. Davis*[,†,⊥]

[†]ARC Centre of Excellence in Convergent Bio-Nano Science and Technology, Monash Institute of Pharmaceutical Sciences, Monash University, Parkville, VIC 3052, Australia

[‡]Children's Cancer Institute, Lowy Cancer Research Centre, Randwick, NSW 2031, Australia

[§]ARC Centre of Excellence in Convergent Bio-Nano Science and Technology, and Australian Centre for NanoMedicine, UNSW Australia, NSW 2052, Australia

[∥]Drug Discovery Biology Theme, Monash Institute of Pharmaceutical Sciences, Monash University, Parkville, VIC 3052, Australia

[⊥]Department of Chemistry, University of Warwick, Coventry, ULCV4 7AL, United Kingdom

Supporting Information

ABSTRACT: Hydrogen sulfide (H_2S) is involved in a myriad of cell signaling processes that trigger physiological events ranging from vasodilation to cell proliferation. Moreover, disturbances to H_2S signaling have been associated with numerous pathologies. As such, the ability to release H_2S in a cellular environment and stimulate signaling events is of considerable interest. Herein we report the synthesis of macromolecular H_2S donors capable of stimulating cell signaling pathways in both the cytosol and at the cell membrane. Specifically, copolymers having pendent oligo(ethylene glycol) and benzonitrile groups were synthesized, and the benzonitrile groups were subsequently transformed into primary aryl thioamide groups via thionation using sodium hydrosulfide. These thioamide moieties could be incorporated into a hydrophilic copolymer or a block copolymer (i.e., into either the hydrophilic or hydrophobic domain). An electrochemical sensor was used to demonstrate release of H_2S under simulated physiological conditions. Subsequent treatment of HEK293 cells with a macromolecular H_2S donor elicited a slow and sustained increase in cytosolic ERK signaling, as monitored using a FRET-based biosensor. The macromolecular donor was also shown to induce a small, fast and sustained increase in plasma membrane-localized PKC activity immediately following addition to cells. Studies using an H_2S-selective fluorescent probe in live cells confirmed release of H_2S from the macromolecular donor over physiologically relevant time scales consistent with the signaling observations. Taken together, these results demonstrate that by using macromolecular H_2S donors it is possible to trigger spatiotemporally confined cell signaling events. Moreover, the localized nature of the observed signaling suggests that macromolecular donor design may provide an approach for selectively stimulating certain cellular biochemical pathways.

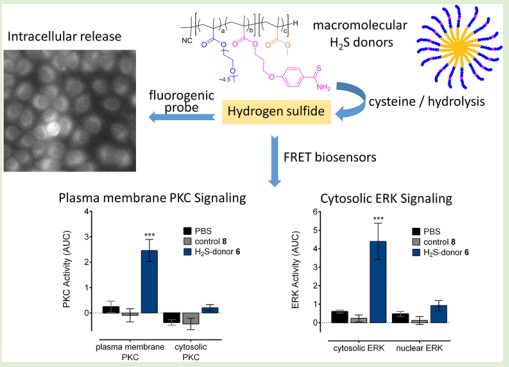

INTRODUCTION

For centuries hydrogen sulfide (H_2S) was primarily known for its toxicity and malodor. However, in 1996 H_2S was identified as having an important physiological function in the nervous system.[1] Since this initial report, many studies have confirmed the endogenous generation of H_2S in the human body and its ability to affect a variety of physiological processes, particularly through participation in signaling cascades.[2−5] H_2S is now considered to be the third member of the gasotransmitter family, along with nitric oxide (NO) and carbon monoxide (CO). As such, H_2S has undergone something of an image transformation from poison and pollutant to important molecule with possible therapeutic potential.[6]

In mammals, endogenous production of H_2S occurs enzymatically in tissues such as vasculature, heart, liver, kidney and brain. Specifically, H_2S is produced through metabolism of L-cysteine (L-cys) under the action of three enzymes: cystathionine-γ-lyase (CSE), cystathionine β-synthase (CBS), and 3-mercaptopyruvate sulfur transferase (3-MST).[7−9] H_2S can also be generated in vivo through nonenzymatic processes, in particular, from sources such as inorganic and organic polysulfides, such as those present in garlic.[10]

One of the best characterized physiological effects of H_2S is the relaxation of vascular smooth muscle cells through H_2S-mediated K_{ATP} channel opening.[11,12] Other studies have suggested that the production of H_2S provides a protective

Received: November 1, 2015
Revised: December 9, 2015

DOI: 10.1021/acs.biomac.5b01469
Biomacromolecules XXXX, XXX, XXX−XXX

effect in some pathologies. For instance, H_2S has been associated with inhibition of leukocyte adherence in the microcirculation during vascular inflammation,[13,14] cardioprotective,[15−17] neuroprotective,[18−20] and gastroprotective effects,[21] regulation of insulin release[22] and promotion of wound healing.[23] A correlation between low levels of H_2S and H_2S-generating enzymes has also been noted in hypertension, Alzheimer's disease, and gastric mucosal injury.[24] Exogenous delivery of H_2S may therefore be a useful strategy in the management of a number of diseases.

The array of physiological processes affected by H_2S is indicative of its participation in a variety of cell signaling pathways such as those involving intracellular mitogen-activated protein (MAP) kinases. For instance, exogenous H_2S was shown to suppress the proliferation of cultured rat aortic vascular smooth muscle cells through the MAPK pathway in a dose-dependent fashion;[25] endogenous and exogenous H_2S was found to upregulate p38 MAPK activity in cultured human umbilical vein endothelial cells;[26] and H_2S treatment of pigs subjected to coronary artery occlusion and reperfusion was found to be associated with higher phosphorylation of the MAPK extracellular signal-regulated kinase (ERK) 1/2.[27] Further, exogenous H_2S was found to promote the survival of human granulocytes, associated with the inhibition of p38 MAP kinase phosphorylation[28] and with the attenuation of lipopolysaccharide (LPS)-induced p38 MAPK phosphorylation in BV-2 microglial cells[29] and keratinocytes.[30]

The potential to deliver H_2S to tissues as a therapy is complicated by its gaseous, toxic, and malodorous nature. Effective delivery to cells must take into account both the rate of production and transient concentration so as to prevent any adverse effect arising from excessive production/concentrations. To date, inorganic sulfide salts (e.g., Na_2S and NaSH) that form HS^- and H_2S immediately upon solvation in buffer have been widely used as H_2S-releasing molecules for biological studies. While sulfide salts have the advantage of rapidly increasing H_2S concentration, this same rapid release of H_2S can result in loss from solution (by volatilization and/or transport across membranes), shortening the effective residence time in tissues.[31] Consequently, the instantaneous delivery of H_2S from inorganic sulfide salts does not reproduce the effects of continuous and controlled biosynthesis. As such, there is a need for a system that mimics the controlled biosynthetic release of H_2S, with an extended time of delivery and in a physiologically relevant concentration range.[32]

With these issues in mind, medicinal chemists have developed organic donor drugs with the intent of reducing the rate of H_2S release and avoiding the transient H_2S concentration surge associated with the sulfide salts.[33,34] Currently, there is considerable research in this area, particularly with respect to the development of hybrid drugs incorporating both H_2S donating molecules and nonsteroidal anti-inflammatory drugs (NSAIDs).[32,35] A number of H_2S-releasing molecules are based on aryl dithiole-3-thione (ADT), especially ether derivatives (ADT-OR)), and these are thought to release H_2S via slow hydrolysis. Further, macromolecular conjugates incorporating ADT−OH have emerged in the last couple of years, and these materials offer several potential benefits over their small molecule analogues.[36,37] Incorporating the drug into a macromolecular conjugate can serve many functions: solubility enhancement for an otherwise hydrophobic drug;[38] improvement of the pharmacokinetic profile of the drug by increasing plasma half-life and volume of distribution and by reducing clearance by the kidneys or liver;[39] and protection of the drug against degradation via hydrolysis or oxidation.[40] In the specific case of ADT−OH, conjugation with hydrophilic poly(ethylene glycol) via an ether bond minimized the toxic side effects of ADT−OH in murine macrophages without impairing its H_2S-releasing properties.[36] A different approach to release H_2S from a macromolecular construct has been to use thiols to activate the release of H_2S from the organic donor.[41−46] This approach has been investigated using methacrylate prepolymers bearing pendent benzaldehyde functionalities.[47] Subsequent side-chain derivatization with different *S*-benzoylthiohydroxylamines resulted in thiooxime functionalized polymers, which could undergo L-cys and glutathione-triggered release of H_2S, consistent with small molecule *S*-benzoylthiohydroxylamines.[45]

In the present study, we explored the synthesis and application of thiobenzamide-functionalized polymers as macromolecular H_2S donors and demonstrated that these materials are effective at stimulating certain cell signaling cascades which are dependent on the liberation of H_2S. Thiobenzamide derivatives (also known as aryl thioamides) have previously been explored as small molecule H_2S-donors, predominantly as hybrid drugs of NSAIDs, which are linked to 4-hydroxy thiobenzamide via an ester bond.[48] Moreover, certain derivatives based on thiobenzamides are thought to release H_2S not only through hydrolysis, but also via reaction with L-cys or glutathione.[43] Most recently, a series of L-lactide copolymers functionalized with different amounts of thiobenzamide units were formed into particles that were found to deliver H_2S over days to weeks.[49] The thiobenzamide moiety, therefore, represents a versatile donor capable of releasing H_2S hydrolytically or via stimulus and in a controlled manner. The incorporation of these moieties into a macromolecular construct offers further advantages as might be expected for a macromolecular therapeutic.

The macromolecular H_2S donors synthesized for the present study possess the ability to form micelles in water, and release H_2S hydrolytically or upon addition of an L-cys trigger. Further, intracellular release of H_2S from the donors was confirmed using a fluorescent probe. FRET-based biosensors were used to confirm that H_2S release from the macromolecular donor could modulate cytosolic ERK signaling and plasma membrane-localized PKC activity within HEK293 cells, without causing any significant toxicity to cells. These results demonstrate that macromolecular H_2S donors are able to trigger spatiotemporally confined cell signaling events, and provide a useful platform for studying the induction of localized cell signaling by application of a macromolecular structure.

EXPERIMENTAL SECTION

Materials. Oligo(ethylene glycol) methyl ether methacrylate (OEGMA) (M_n = 300 g mol^{-1}) and methyl methacrylate (MMA) were purchased from Sigma-Aldrich and passed through a column of basic alumina in order to remove inhibitor before use. Initiators, α,α'-azobis(isobutyronitrile) (AIBN) and 1,1′-azobis(cyclohexanecarbonitrile) (ACHN), were purchased from Sigma-Aldrich and purified by recrystallization from methanol and chloroform/methanol respectively before use. The RAFT agent, 4-cyano-2-propyl benzodithioate (CPBDT) was purchased from Sigma-Aldrich at the highest purity available (>97% HPLC) and used as received. Sodium sulfide (Na_2S) anhydrous was purchased from Alfa Aesar (Cat. No. 65122) and hydrochloric acid 32% was purchased from Ajax Finechem. Solvents (except anhydrous solvents) were purchased from Merck Millipore and used as received.

DOI: 10.1021/acs.biomac.5b01469
Biomacromolecules XXXX, XXX, XXX−XXX

All other chemicals such as reagents and anhydrous solvents for synthesis were purchased from Sigma-Aldrich at the highest purity available and used without further purification (unless otherwise stated). A Reveleris Flash Chromatography System fitted with GRACE silica cartridges was used for purification of monomer and intermediates. TLC was performed on Merck Silica $60F_{254}$ plates.

Characterization. ^{1}H (400 MHz) and ^{13}C NMR (100 MHz) spectra were obtained with a Bruker UltraShield 400 MHz spectrometer at 25 °C running Bruker Topspin Software. Spectra were recorded for samples dissolved in deuterated solvent (chloroform, $CDCl_3$, or dimethyl sulfoxide, DMSO) and chemical shifts are reported as parts per million from external tetramethylsilane. Monomer conversions were obtained from the ^{1}H NMR spectra.

Gel permeation chromatography (GPC) was performed using a Shimadzu modular system comprised of a DGU-12A degasser, an SIL-20AD automatic injector, a 5.0 μm bead-size guard column (50 × 7.8 mm), followed by three KF-805L columns (300 × 8 mm, bead size: 10 μm, pore size maximum: 5000 Å), a SPD-20A ultraviolet detector, and an RID-10A differential refractive-index detector. The temperature of columns was maintained at 40 °C using a CTO-20A oven. The eluent was *N*,*N*-dimethylacetamide (DMAc, HPLC grade, with 0.03% w/v LiBr), and the flow rate was kept at 1 mL/min using a LC-20AD pump. A molecular weight calibration curve was produced using commercial narrow molecular weight distribution polystyrene standards with molecular weights ranging from 500 to 2 × 10^6 g mol^{-1}. Polymer solutions at approximately 2 mg mL^{-1} were prepared and filtered through 0.45 μm filters prior to injection.

Attenuated total reflectance-fourier transform infrared spectroscopy (ATR-FTIR) spectra were obtained using a Shimadzu IR Tracer-100 Fourier transform infrared spectrometer fitted with a GladiATR 10 single reflection accessory. Data was processed using LabSolutions IR software in the mid-IR region of 4000−500 cm^{-1} at a resolution of 8 cm^{-1} by averaging 128 scans (collected via a mercury cadmium tellyuride detector).

Dynamic light scattering (DLS) measurements were carried out on a Malvern Zetasizer Nano ZS Series running DTS software (laser, 4 mW, λ = 633 nm; angle 173°). The polydispersity index (PDI) was used to describe the average diameters and size distribution of prepared micelles from a Cumulants analysis of the measured intensity autocorrelation function. Samples were filtered using 0.45 μm Nylon syringe filter to remove contaminants/dust prior to measurement.

Synthesis. The synthesis and characterization of all small molecules (intermediates, standards, SF4 fluorogenic probe, CPPMA monomer), macromolecules (macromolecular precursors, H_2S donors, and control) and detailed methods that were applied to measure H_2S release time course are fully described in the Supporting Information.

Synthesis of [POEGMA$_{46}$]-S(C═S)Ph (1). The polymerization was carried out using the following stoichiometry of $[CPBDT]_0/[OEGMA]_0/[AIBN]_0$ = 1:80:0.125. OEGMA (2.12 g, 7.08 × 10^{-3} mol), CPBDT RAFT agent (19.4 mg, 8.76 × 10^{-5} mol), AIBN (1.80 mg, 1.10 × 10^{-5} mol), and acetonitrile (ACN; 8 mL) were placed in a round-bottom flask equipped with a magnetic stirrer bar and capped with a rubber septum. The reaction mixture was deoxygenated for 30 min at 0 °C by sparging with N_2. The deoxygenated mixture was placed into a preheated oil bath at 70 °C and the polymerization left to stir for 6 h. The resulting mixture was then allowed to cool in an ice bath for about 15 min to terminate polymerization and then exposed to air. The monomer conversion was determined by ^{1}H NMR. The resonances integrated to obtain conversions for OEGMA polymerizations were the vinyl peaks at 5.4 and 5.9 ppm (monomer only) and the OCH_2− peaks at 3.8−4.1 ppm (monomer and polymer). To remove all traces of unreacted monomer the polymerization solution was first transferred to dialysis tubing (Cellu Sep, nominal MWCO 3500 g mol^{-1}) and dialyzed against acetone with at least five exchanges of solvent. This was followed by multiple precipitation and centrifugation steps, using petroleum ether/diethyl ether 1:1 as the precipitant. Residual solvent was then removed by blowing a gentle stream of nitrogen over the polymer solution overnight, followed by drying with a high vacuum line. The final product, POEGMA$_{46}$-S(C═S)Ph **1**, was analyzed by ^{1}H NMR and GPC. Polymerization results: conversion = 60%; M_n 9672 g/mol, PDI 1.12 (GPC-DMAc); M_n 14020 g/mol (^{1}H NMR estimate); M_n 14620 g/mol (theoretical M_n). The ^{1}H NMR spectrum of **1**, with main peak assignments, is provided as Figure S1.

Synthesis of [POEGMA$_{46}$]-*block*-[PCPPMA$_{10}$-*co*-PMMA$_{99}$]-S(C═S)Ph (4). The polymerization was carried out using the stoichiometry of $[POEGMA\ Macro\ RAFT]_0/[monomers]_0/[AIBN]_0$ = 1:188:0.129. The molar feed ratio of MMA to CPPMA was 9:1. Briefly, POEGMA$_{46}$-S(C═S)Ph (**4**; 0.435 g, 3.10 × 10^{-5} mol), MMA (0.532 g, 5.31 × 10^{-3} mol), CPPMA (0.130 g, 5.31× 10^{-4}), AIBN (0.64 mg, 3.86 × 10^{-6} mol), and anhydrous 1,4-dioxane (1.8 mL) were transferred to a glass vial equipped with a magnetic stirrer bar and capped with a rubber septum. The reaction mixture was deoxygenated with nitrogen for 30 min at 0 °C by sparging with N_2. The deoxygenated solution was then placed into a preheated oil bath at 70 °C and the block copolymerization was allowed to proceed with stirring for 15 h. The polymerization was terminated by placing the sample in an ice bath for 15 min. The monomer conversion was determined by ^{1}H NMR. The resonances integrated to obtain conversions for CPPMA were the CH_2 resonance (triplet) at 4.2 ppm from the CPPMA monomer only versus aromatic peaks at 6.8−7.0 ppm (monomer and polymer). The MMA vinyl peaks at 5.4 and 5.9 ppm (monomer only) could be ascertained, and the average value was compared to a broad resonance at 3.5 ppm corresponding to the methoxy hydrogens of the polymerized MMA. The product polymer was recovered by multiple precipitations into diethyl ether/petroleum ether. The purified block polymer was then dried under high vacuum after evaporating off a majority of the solvent with a stream of nitrogen. The final product [POEGMA$_{46}$]-*block*-[PCPPMA$_{10}$-*co*-PMMA$_{99}$]-S(C═S)Ph **4** was analyzed by ^{1}H NMR and GPC. Polymerization results: conversion (CPPMA) = 50%; conversion (MMA) = 50%; M_n 19850 g/mol, PDI 1.14 (GPC-DMAc); M_n 26400 g/mol (^{1}H NMR estimate); M_n 25500 g/mol (theoretical M_n). The ^{1}H NMR spectrum of **4** with peak assignments is provided as Figure S2. Overlayed GPC traces showing block extension are displayed in Figure S3.

RAFT End Group Removal from [POEGMA$_{46}$]-*block*-[PCPPMA$_{10}$-*co*-PMMA$_{99}$]-S(C═S)Ph (4). A solution of [POEGMA$_{46}$]-*block*-[PCPPMA$_{10}$-*co*-PMMA$_{99}$]-S(C═S)Ph, **4** (0.430 g, 1.63 × 10^{-5} mol, 1 equiv), 1-ethylpiperidine hypophosphite (EPHP; 0.030 g, 1.70 × 10^{-4}, ∼10 equiv), AIBN (1.0 mg, 6.09 × 10^{-6}, 0.37 equiv), and anhydrous toluene (3.0 mL) were added to a Schlenk vessel with a magnetic stirrer bar and capped with a rubber septum. The reaction mixture was deoxygenated with nitrogen for 30 min and then placed into a preheated oil bath at 80 °C with stirring for 2 h. The radical-induced reduction process was terminated by placing the sample in an ice bath for 15 min. The product was then recovered by multiple precipitations into diethyl ether/petroleum ether (1:2). After drying under a stream of nitrogen, the conversion for thiocarbonylthio end group removal was determined by ^{1}H NMR to be only 90%. The procedure was therefore repeated, as described above. However, after precipitation and drying the product was found to contain reaction byproducts, most likely from EPHP. These were removed by washing the polymer, dissolved in chloroform, with water and brine. Decolorization of the polymer and ^{1}H NMR analysis showed that the RAFT end groups and reaction byproducts had been adequately removed. Specifically, three distinct signals in the ^{1}H NMR spectrum (δ 7.35, 7.50, and 7.90 ppm), representing the aromatic benzodithioate, were found to be removed on radical-induced reduction. The final product was also analyzed by GPC to monitor possible side reactions such as termination. Results: conversion > 95%; M_n 22014 g/mol, PDI 1.15 (GPC-DMAc). The ^{1}H NMR spectrum before and after RAFT end group removal is provided as Figure S4.

Thionation of [POEGMA$_a$]-*block*-[PCPPMA$_b$-*co*-PMMA$_c$]-H To Give [POEGMA$_a$]-*block*-[PTHA$_b$-*co*-PMMA$_c$]-H (7). [POEGMA$_a$]-*block*-[PCPPMA$_b$-*co*-PMMA$_c$]-H (0.320 g) from the previous step was dissolved in anhydrous DMF (2 mL), followed by the successive addition of magnesium chloride hexahydrate ($MgCl_2{\cdot}6H_2O$; 120 mg, 5.90 × 10^{-4} mol) and 70% sodium hydrosulfide hydrate (100 mg, 1.2 × 10^{-3} mol). The green slurry was left to stir at room temperature for

DOI: 10.1021/acs.biomac.5b01469
Biomacromolecules XXXX, XXX, XXX−XXX

Scheme 1. Synthesis of CPPMA Monomer, Precursor Polymers, 2a, 3, and 4, and Subsequent Conversion to Thioamide Polymers 5, 6, and 7[a]

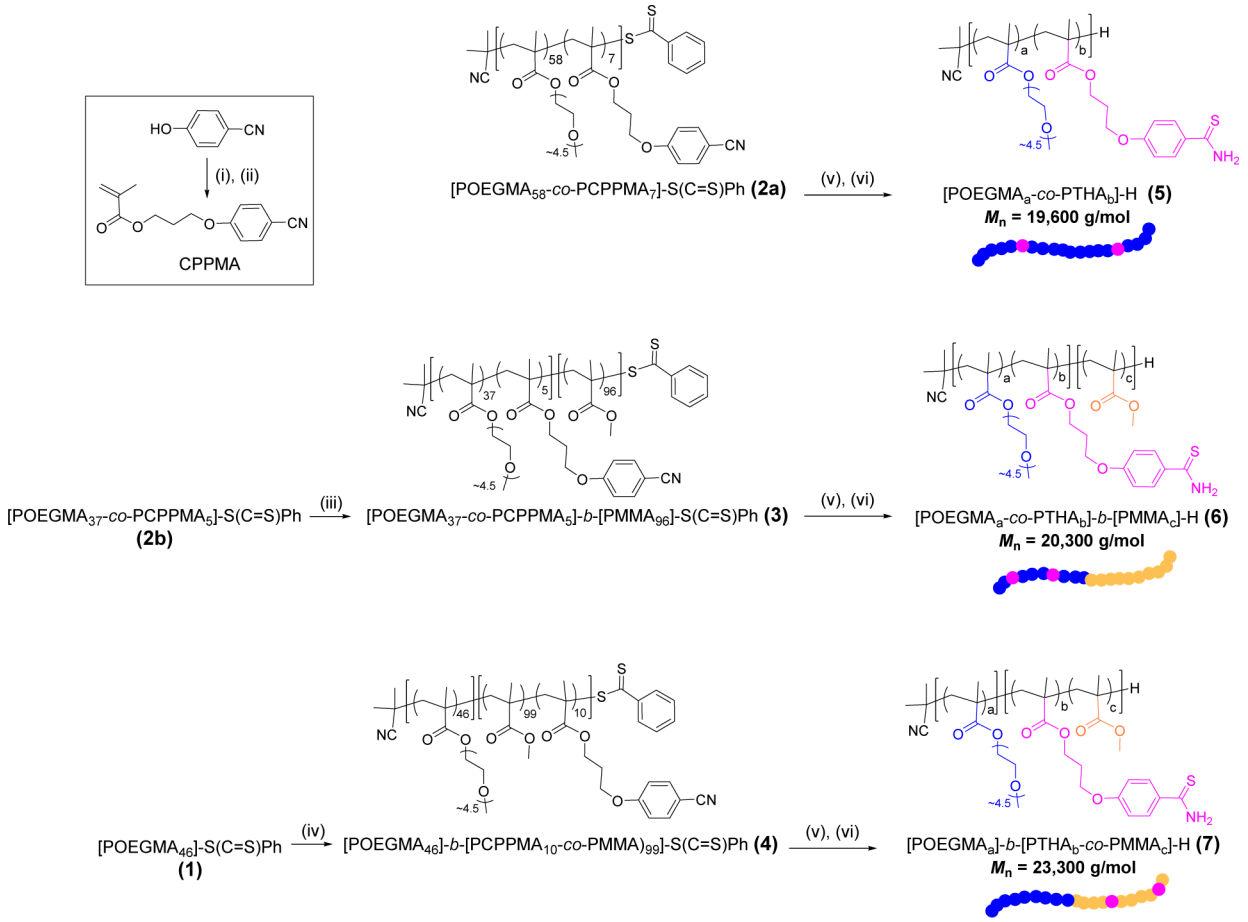

[a]Reagents and conditions: (i) 3-bromo-1-propanol, K_2CO_3, and DMF; (ii) methacrylic anhydride, TEA, and DCM; (iii) MMA, 70 °C, 1,4-dioxane; (iv) MMA, CPPMA, 70 °C, 1,4-dioxane; (v) polymer end-group removal, 1-ethylpiperidine hypophosphite, AIBN, toluene, 80 °C; (vi) thionation, NaHS, DMF, $MgCl_2 \cdot 6H_2O$. CPPMA = 3-(4-cyanophenoxy) propyl methacrylate; OEGMA = oligo(ethylene glycol) methyl ether methacrylate, with average M_n = 300 g/mol; MMA = methyl methacrylate.

4 h. The slurry was then added to 0.2 M aqueous HCl (5 mL), and the resulting yellow gum was stirred for several minutes. The crude product was then extracted using chloroform and washed with 0.2 M HCl (×2), water (×2), and saturated brine (×1). The organic phase was then dried with $MgSO_4$ (anhydrous) and the solvent was removed under reduced pressure, leaving behind a yellow glassy polymer. The final product [$POEGMA_a$]-*block*-[$PTHA_b$-*co*-$PMMA_c$]-H, 7, was also analyzed by GPC to monitor possible side reactions and termination. Results: M_n 23300 g/mol, PDI 1.16 (GPC-DMAc). The ^1H NMR spectrum before and after thionation is provided as Figure S5.

Biological Evaluation of H_2S Donating Polymer ***6***. Preparation of macromolecular solutions: Micelle solutions of polymers (macromolecular control **8** and macromolecular H_2S-donor **6**) were prepared ∼1 h prior to cell experiments, by dropwise addition of the polymer dissolved in THF (10 mg/mL THF) into nitrogen-sparged PBS pH 7.4 (10 mg of polymer solution/10 mL PBS). The THF was then removed using a centrifugal filter unit (Amicon Ultra-4, Ultracell-3K, regenerated cellulose 3000 NMWL). For this, an aliquot of micelle solution (500 μL) underwent three spin cycles of 20 min each at 5000−6000 rpm. The solution was reconstituted to the original volume with nitrogen-sparged PBS 7.4 after each spin cycle. The final concentration of micelle solution was 1 mg/mL. For the high-content ratiometric FRET imaging experiments and high-content SF4 time course studies, the micelle solutions were diluted 1:10 in PBS prior to addition to the cells (final concentration 0.1 mg/mL). For the intracellular H_2S release imaging studies (using SF4 probe), the micelle solutions were diluted 1:1 in OptiMEM prior to addition to the cells (final concentration 0.5 mg/mL).

Cell Culture for High-Content Ratiometric FRET and SF4 Time-Course Study. HEK293 cells were grown in DMEM supplemented with 5% v/v FBS, and all assay plates were coated with poly-D-lysine (5 μg/cm^2) prior to use.

High-Content Ratiometric FRET Imaging. HEK293 cells were seeded in black, optically clear 96-well plates and grown to 70% confluency prior to transfection with 90 ng/well FRET biosensor using linear polyethylenimine (PEI).[50] NucEKAR Cerulean-Venus (Addgene plasmid 18681) and cytoEKAR Cerulean-Venus (Addgene plasmid 18679) were gifts from K. Svoboda.[51] CytoCKAR (Addgene plasmid 14870) and pmCKAR (MyrPalm-CKAR, Addgene plasmid 14862) were gifts from A. Newton.[52,53]

At 48 hours following transfection, fluorescence imaging was performed using a high-content GE Healthcare INCell 2000 Analyzer with a Nikon Plan Fluor ELWD 40× (NA 0.6) objective and FRET module, as described previously.[54] For CFP/YFP (cytoCKAR, pmCKAR) or Cerulean/Venus (nucEKAR, cytoEKAR) emission ratio analysis, cells were sequentially excited using a CFP filter (430/24) with emission measured using YFP (535/30) and CFP (470/24) filters, and a polychroic optimized for the CFP/YFP filter pair (Quad3). HEK293 cells were imaged every 90 s (image capture of 20 wells per 90 s). Baseline signaling was measured in cells over 6 min, followed by the addition of polymer (either macromolecular control **8** or macromolecular H_2S-donor **6**) or PBS, and the response was

DOI: 10.1021/acs.biomac.5b01469
Biomacromolecules XXXX, XXX, XXX−XXX

measured over 1 h. For all wells, a positive control for signaling (used to generate a maximal increase in the signaling pathway: 200 nM phorbol 12,13-dibutyrate (PDBu) for ERK or 200 nM PDBu with phosphatase inhibitor cocktail for PKC) was measured to allow only cells that responded to the positive control to be selected for analysis. Data were analyzed using in-house scripts written for the FIJI distribution of ImageJ,[55] as described previously.[54] Data are expressed as the mean ± SEM from 170 to 292 cells.

Preparation of Solutions of SF4. These were prepared fresh in DMF/DMSO (5 mM) and diluted to give a 5 μM solution in Hank's Balanced Salt Solution (HBSS) for the high-content SF4 time course study or in OptiMEM for the intracellular H_2S release imaging studies.

High-Content SF4 Time-Course Study. HEK293 cells were seeded in triplicate in black, optically clear 96-well plates and grown to 90% confluency. Cells were washed once with HBSS and nuclei were stained using Hoechst nuclear stain 33342 for 10 min at 37 °C. Fluorescence imaging was performed using a high-content PerkinElmer Operetta with an Olympus LUCPlanFLN 20× (NA 0.45) objective. Nuclei were visualized using the Hoechst 33342 filter set (excitation 360−400, emission 410−480), and SF4 fluorescence was visualized using the EGFP filter set (excitation 460−490, emission 500−550). Images were taken every 2 min.

Cells were washed with HBSS, then loaded with 5 μM SF4 probe (in HBSS) for 10 min at 37 °C. Baseline fluorescence was determined for 8 min followed by the addition of the macromolecular H_2S-donor **6** (or macromolecular control **8**), then images were taken every 2 min for 1 h at 37 °C. Data were automatically analyzed by determining the mean SF4 fluorescence per well using Harmony High Content Imaging and Analysis software (v3.5.2). SF4 fluorescence was PBS vehicle-subtracted and expressed relative to the baseline fluorescence for each experimental condition. Data are expressed as the mean ± SEM from three independent experiments.

Cell Culture for Intracellular Imaging of H_2S Release Using SF4 Probe. H460 lung carcinoma cells were maintained in T75 flasks in exponential growth as a monolayer in DMEM (Gibco by Life Technologies) supplemented with 10% fetal bovine serum and 1% L-glutamine, and incubated at 37 °C in 5% CO_2. Cells were plated into poly-D-lysine-coated μ-dishes (ibidi, 35 mm) at 20000 cells per dish and allowed to attach for 3 days.

Intracellular Imaging of H_2S Release Using SF4 Probe. On the day of imaging, the culture medium was removed and cells were washed with PBS once. Cells were treated with freshly prepared micelle solutions (macromolecular control **8** or macromolecular H_2S-donor **6**) diluted 1:1 with OptiMEM for 60 min, followed by 1 μM Hoechst nuclear stain 33342 for 10 min prior to imaging. The micelle solution was removed and the cells were washed with PBS once. The cells were then incubated with 5 μM SF4 (H_2S probe) and images were collected at 5 min intervals using a Nikon Eclipse Ti-E microscope. The cells were excited using a GFP filter cube for SF4 fluorescence and a DAPI cube for H33342 nuclear stain.

RESULTS AND DISCUSSION

Synthesis of Macromolecular H_2S Donors. Thioamides and their derivatives are an important class of molecules due to their use in synthetic chemistry, especially in the preparation of sulfur-containing heterocycles such as thiazoles and thioazolines.[56] Their utility stems in part from the presence of both nucleophilic and electrophilic reactive centers in their structures. In this work we employed the reversible addition−fragmentation chain transfer (RAFT) polymerization technique to synthesize macromolecular structures. Since thioamides are also known to undergo photochemical radical reactions,[57] rather than directly polymerizing a thioamide functionalized monomer into our structures, which could potentially degrade during the polymerization, we employed a postpolymerization approach. This involved copolymerization of a monomer bearing a benzonitrile group which could subsequently be converted in high yield into a primary aromatic thioamide. We anticipated that benzonitrile groups would remain inert to radicals during the polymerization, making them ideal candidates for the postpolymerization modification strategy.

The monomer 3-(4-cyanophenoxy)propyl methacrylate (CPPMA; Scheme 1), which is not commercially available, was synthesized in two steps from 4-cyanophenol. First, 4-cyanophenol was alkylated with 3-bromo-1-propanol, after which the aliphatic alcohol was esterified with methacrylic anhydride. Somewhat inconveniently, the monomer was found to form large insoluble crystals on standing. This is not surprising, considering that the acrylic version has been applied in dispersed liquid crystal polymerizable compositions due to its ability to elicit phase separation and structural ordering.[58] This crystallization phenomenon was circumvented by keeping the monomer dissolved in solvent with a small amount of inhibitor, with isolation only executed immediately prior to use.

The monomer was incorporated into 3 types of polymer precursors, **2a**, **3**, and **4**, as shown in Scheme 1, using the RAFT agent, 4-cyano-2-propyl benzodithioate (CPBDT). First, it was copolymerized with oligo(ethylene glycol) monomethyl ether methacrylate ($OEGMA_{300}$) to give hydrophilic POEGMA-*co*-PCPPMA copolymers **2a** and **2b**. Copolymer **2a** was used as prepared, while **2b** was block extended with methyl methacrylate (MMA) to give block copolymer **3**. CPPMA was also copolymerized with MMA in a block extension step from POEGMA **1**, to give block copolymer **4**. Block copolymers **3** and **4** differed in that the CPPMA was incorporated into either a soft hydrophilic or rigid hydrophobic block, accounting for ∼10% of the block molar content in both. Each of the block copolymers were synthesized with a view to forming self-assembled micelles in PBS at pH 7.4. For POEGMA-*co*-PCPPMA **2a** (which was not block extended), the CPPMA accounted for ∼10% of the copolymer content. However, the lack of a hydrophobic segment means that final copolymer **2a** would only be able to form unimers in PBS at pH 7.4, as opposed to self-assembled micelles. The polymerization characteristics for the benzonitrile copolymers, which are expected to contain random distributions of pendent CPPMA units along each polymer chain, are shown in the Supporting Information (SI, Table S1).

Following successful synthesis of the precursors, benzonitrile groups in the polymers were converted into primary aromatic thioamide moieties, often referred to in the literature as thiobenzamides. Initially, we tested the reagent commonly used for this thionation (or thiolysis) reaction, Lawesson's reagent, but found conversions to be low. Hydrogen sulfide gas, another commonly used reagent, was not considered due to the high bubbling rates and pressures required owing to its low solubility in organic solvents, combined with its hazardous nature. Instead, thioamide formation as a postpolymerization modification reaction was carried out using sodium hydrosulfide (NaHS, ∼ 70%) and $MgCl_2.6H_2O$ in DMF (as in Scheme 1).[59] Initial trials using this method gave high conversions to thioamide, although this was found to be concurrent with RAFT (benzodithioate) polymer end group removal. The latter was apparent by the immediate decolorisation of the polymer. NaHS has been briefly studied as a nucleophilic agent for the conversion of RAFT agents into thiols so this outcome was not unexpected.[60] However, due to reactivity of the thioamides to thiols, we decided to remove the RAFT end groups before carrying out the thionation reaction. Therefore, diblock copolymers **3** and **4**, as well as copolymer **2a**, were subjected to a radical-induced reduction using *N*-ethylpiperidine hypo-

DOI: 10.1021/acs.biomac.5b01469
Biomacromolecules XXXX, XXX, XXX−XXX

phosphite (EPHP) and a thermal initiator, to give a hydrogen end group.[61] Other than decolorization of the polymer, this was evidenced by the loss of three distinct signals in the ^{1}H NMR spectrum (δ 7.4, 7.5, and 7.9 ppm), which corresponded to the aromatic benzodithioate end group protons (SI, Figures S4, S9, and S12). The GPC traces for the polymers after end group removal were found to broaden marginally, due to the formation of higher molecular weight polymer species (Figures S3, S8, and S14).

The thionation reaction conditions were found to convert benzonitrile groups to thioamides almost completely within 4 h. Shorter reaction times and exclusion of $MgCl_2{\cdot}6H_2O$ caused conversions to diminish. We did not monitor conversions over time, mainly due to the complex work up and small quantities of polymer employed. An alternative method was trialed using pyridine as a solvent, triethylamine, and a 20% solution of ammonium sulfide in water,[62] however, this gave poor yields of thioamide.

In order to ascribe peaks in the final ^{1}H NMR spectra and subsequent FTIRs, we synthesized a control molecule, 4-butoxybenzothioamide. Representative ^{1}H NMR spectra (collated as Figure 1) show changes in the aromatic protons

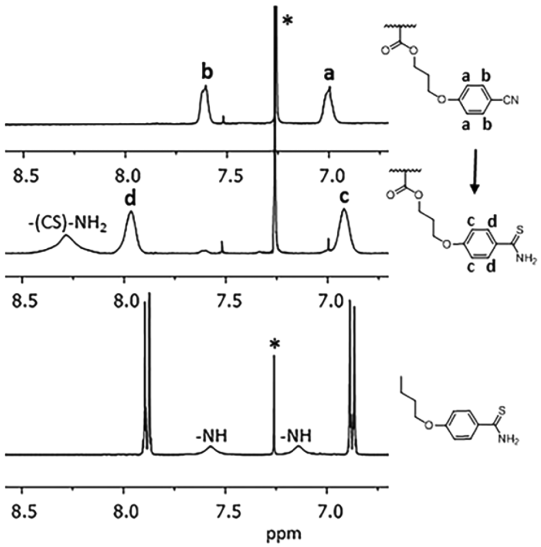

Figure 1. ^{1}H NMR spectra (400 MHz, $CDCl_3$) showing the aromatic proton signals for polymer **3** with the RAFT end group removed before (top) and after (**6**, middle) the thionation process vs control molecule 4-butoxybenzothioamide (bottom).

for block copolymer **3** (with RAFT end group removed), after the thionation process, as compared to the control molecule. It is worth noting that the NH_2 groups of the pendent thioamide moieties in polymer **6** were shifted versus the control molecule, which could be the result of hydrogen bonding with other units along the chain, such as OEGMA units. Solid-state ATR-FTIR spectra for the control thioamide molecule (Figure S17) and the intermediate, 4-(3-hydroxypropoxy)benzonitrile (Figure S18) display characteristic transmission peaks from thioamide (i.e., 3130−3300 cm^{-1} (NH_2 bands) and 1630 cm^{-1} (C−N and N−H combined stretching)) and from the benzonitrile (2226 cm^{-1} (−C≡N stretching)). These characteristic peaks are clearly distinguished in the ATR-FTIR spectra of macroRAFT **2a** and thionated polymer **5** (Figure S20). As further evidence of successful thionation, all polymers developed a yellow color after the reaction, such color being characteristic for thioamides.[63]

The composition of polymers did not change markedly on thionation (Table S2), indicating that the pendent ester groups along the chain were not significantly susceptible to reaction with HS^- ions during the thionation process nor during workup. Moreover, there was no evidence of −COSH protons in our ^{1}H NMRs (the signal of the thiol protons of thioacetic acid $CH_3COS\underline{H}$ appears at 4.6 ppm in $CDCl_3$). While GPC traces were found to broaden somewhat during the RAFT end group removal process, this was not observed for the thionation step, suggesting that oxidized thiols did not form along the chains (Figures S3, S8, and S14).

Since the polymer end groups were no longer visible in the ^{1}H NMR spectrum, we used the GPC-derived molecular weights for subsequent calculations that required molecular weight estimates of the thionated polymers (**2a**, **6**, and **7**). These are displayed in Scheme 1 (as well as in Table S2). With thionation conversions >95% for each polymer, the number of benzonitrile groups in the original RAFT end functional polymers was used to approximate the number of thioamide units in the final polymers. We used these values to calculate the concentration of thioamides in the testing solution and thereby assess the H_2S-donating ability of each polymer.

Finally, each polymer was tested for its capacity to form micelles (Figure S15). A total of 10 mg of block copolymer (either **6** or **7**) was dissolved in 1,4-dioxane (1 mL). Subsequent micelle formation was afforded by injecting 10 mL of PBS (pH 7.4) into the polymer−dioxane solution under vigorous stirring at room temperature. Block copolymer **6** afforded 18 nm micelles, and block copolymer **7** afforded 25 nm micelles by DLS. Copolymer **5** was prepared the same way and gave unimers in solution.

Assessment of H_2S-Releasing Ability. The capacity of the synthesized polymers to function as macromolecular H_2S donors was examined using an amperometric approach using an H_2S selective microsensor, with a working concept published by Jeroschewski et al.[64] The H_2S-selective and calibrated microsensor was used to measure the evolution of H_2S concentration (μmol/L) over time in solutions of polymers **5**, **6**, and **7** in PBS at pH 7.4. Additionally, thiol-triggered release was measured after an aliquot of L-cys had been added to the solution (22 °C). Figure 2 shows H_2S concentration produced over time for the H_2S-donating polymers, with and without addition of L-cys.

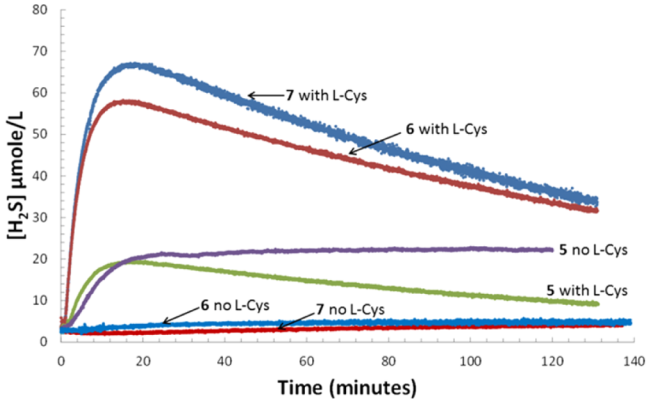

Figure 2. Representative H_2S release curves for polymers (10 mg), as measured by the amperometric microsensor method (PBS at pH 7.4, 10 mL), L-Cysteine (400 mM, 100 μL aliquot).

DOI: 10.1021/acs.biomac.5b01469
Biomacromolecules XXXX, XXX, XXX−XXX

Table 1. Release Characteristics of Thioamide Polymers, as Measured Using Amperometry

polymer	L-cys[a] (Y/N)	peaking time[c] (min)	peaking $[H_2S]$[b] (μmol/L)	$[sulfides]_{tot}$[d] (μmol/L)	[thioamides][e] (μmol/L)	sulfides (MPC) released[f] (%)
7	Y	14	67	226	390	58
7	N	>120	3	10	390	3
6	Y	13	58	196	224	88
6	N	60	4	19	224	8
5	Y	12	19	64	325	20
5	N	41	23	78	325	24

[a]Y = L-cysteine added (400 mM, 100 μL aliquot) during microsensor recording; N = L-cysteine not added. [b]Highest μmol/L H_2S value attained on the curve of $[H_2S]$ vs time. [c]Time taken to reach highest value of μmol/L on the curve of $[H_2S]$ vs time. [d]Total sulfides concentration = $[sulfides]_{tot}$ = $[H_2S]$ + $[HS^-]$, where $[sulfides]_{tot}$ = $[H_2S] \times (10^{pH-pK1} + 1)$ = 3.40 × $[H_2S]$ (see Supporting Information for explanation of equations). [e]$[Thioamides] = n(thioamides)/0.011$, where 11 mL = total volume in reaction vessel for microsensor testing; n(thoamides) = (average number of units in each chain) × n(polymer); average number of units in each chain is taken to be equal to number of CPPMA units in the original polymers and $n(polymer) = 0.01/M_n$ (GPC, DMAc) since 10 mg of polymer was tested. [f]% sulfides released (measured at peaking concentration) = $[sulfides]_{tot}/[thioamides]$.

Considerations for H_2S-Releasing Ability of Polymers. To obtain a reasonable estimation of H_2S release kinetics across the series **5**–**7**, we compared peaking time, which is the time taken to reach the maximum $[H_2S]$ value in solution and the peak value of $[H_2S]$. These values are provided in Table 1, columns 3 and 4, respectively. Importantly, in order to make relative assessments of H_2S donation across the polymeric series, several issues needed to be taken into consideration, related to the establishment of an ionization equilibrium between H_2S and HS^-.[65] Such aspects, which are defined further in the Supporting Information, can be simplified into the total concentration of dissolved sulfide species generated in solution: $[sulfides]_{tot} = [H_2S] + [HS^-]$, which can be calculated from

$$[sulfides]_{tot} = [H_2S] \times (10^{pH-pK_1} + 1) \quad (1)$$

The amperometric sensor only detects partial pressure of H_2S and since the test is carried out in pH 7.4 buffer, this only accounts for one component of the total sulfides, $[sulfides]_{tot}$, generated. Using eq 1, one can estimate $[sulfides]_{tot}$ existing in solution at pH 7.4:

$$[sulfides]_{tot} = [H_2S]_{measured} \times 3.40$$

The derived peaking value of $[sulfides]_{tot}$ for each polymer is provided in Table 1, column 5. A further measure of the H_2S-generating capability of the polymers was made based on a comparison of peaking value of $[sulfides]_{tot}$, with the concentration of thioamide groups originally present in the testing solution. The polymers were tested for H_2S release at a concentration of 10 mg/11 mL of solution (to guarantee micellization for block copolymers), resulting in different starting concentrations of thioamide in the measurement solution. Furthermore, the amperometric probe measures H_2S in real time and is not a cumulative measure of dissolved gas. Consequently, loss of H_2S over time due to volatilization (both to the headspace and escape from the measurement vessel), and oxidation due to oxygen in the system cannot be overlooked in our experiments, as these phenomena could result in a reduction in the amount of H_2S measured in solution. This means that the peaking concentration may never approximate total sulfides released from each thioamide polymer, and therefore, a comparison of the two values may not be entirely a measure of % sulfides released. This value is therefore more appropriately expressed as % sulfides measured at peaking concentration (% sulfides (MPC)), which allows some comparative assessment to be made of the H_2S-releasing capability of each of the polymers. These values are given in Table 1, column 7.

H_2S-Releasing Ability of Polymers. In the absence of L-cys, thioamides release H_2S via a hydrolysis mechanism, a process that is promoted by acid or base. This is analogous to the hydrolysis of thioacetamide, which leads to the corresponding amide.[66,67] Aromatic thioamides are more likely to undergo this mechanism due to their aromatic ring, which stabilizes intermediates. Figure 2 shows the curves of H_2S concentration over time for the various polymers, both with and without L-cys. The hydrolysis rates leading to H_2S release (i.e., with no L-cys present) were found to be low overall, with the fastest release of H_2S measured for water-soluble copolymer **5**, which forms unimers in solution (41 min). This was followed by micelle-forming polymer **6** (60 min), which incorporated thioamides in the hydrophilic corona, followed by micelle-forming polymer **7** (>120 min), which incorporates thioamides in the hydrophobic core. These results are anticipated for a hydrolysis mechanism, since this route involves charged intermediates that are stabilized by solvation with water. This is likely to be less favored in an aggregated and hydrophobic environment, such as the core of a micelle (i.e., as in **7**).

With respect to the peaking value of $[sulfides]_{tot}$ generated on hydrolysis, copolymer **5** ranked the highest (78 μM). With respect to the concentration of thioamides originally present in solution, this material released approximately 24%. In contrast, micelle forming polymers **6** and **7** showed lower levels of release. Polymer **6**, with thioamides in the hydrophilic corona, gave a slightly higher release value (8%) compared to polymer **7** (3%). The different levels of H_2S released from unimer-forming polymer **5** and micelle-forming polymer **6** (in which thioamides reside in the corona) is worth noting. In both of these cases, one would envisage similar hydrated environments. However, the aromatic nature of the thioamide itself may result in some partitioning of units within the core of the micelle to promote some stacking or aggregation, factors that could reduce hydrolysis of thioamides in **6**. Even though hydrolysis led to low levels of H_2S release overall, the results suggest that a nonaggregated polymeric system (as in **5**) promotes hydrolysis of thioamides more so than do aggregated systems **6** and **7**.

The exact mechanism of L-cys triggered release from thioamides is not known to us, and a survey of literature uncovered little with respect to the aqueous reaction of thiols with thioamides. In transamidation, primary amines can replace the sulfur of the thioamide with an amine residue (with formation of *N*-substituted amidines) to release H_2S.[68] We do

DOI: 10.1021/acs.biomac.5b01469
Biomacromolecules XXXX, XXX, XXX−XXX

not believe that this is the route to H_2S release from our materials, since the amine group of L-cys exists predominantly as the positively charged α-ammonium ion ($-NH_3^+$) at pH 7.4 and, thus, has reduced nucleophilic capacity. Furthermore, we found that we could trigger the release of H_2S from polymer **7** using the *N*-protected thiol amino acid, *N*-acetyl-D-penicillamine (results not shown). Calderone et al.[43] also report glutathione-triggered release from arylthioamides, which is highly suggestive of a thiol-triggered process.

As is evident in Figure 2, for all the polymers tested, the rate of thiol-triggered H_2S release was found to be greater than that by hydrolysis (12−14 min until peaking for the series), indicating that it is generally a faster reaction. The thiol-triggered peaking H_2S concentrations, however, were found to be markedly higher (at least 10× higher) than the corresponding concentrations for hydrolysis in the case of micelle forming polymers **6** and **7**. For unimer-forming copolymer **5**, peaking concentrations were found to be almost equivalent for both hydrolysis and thiol-triggered release. Further, when taking into consideration the concentration of thioamides originally present in solution, copolymer **5** was found to release the smallest amount (20%) versus polymers **6** and **7**, which achieved higher values (88 and 58%, respectively). We cannot discount a possible hydrolysis mechanism that does not result in H_2S and, further, that this could explain the lower quantities of H_2S released for polymer **5**, which underwent hydrolysis more so than **6** and **7**. Some H_2S could have also been lost to hydrolysis during the addition of polymer **5** (in dioxane) to the water solution or possibly even due to absorption of water on standing and during the work-up stage, which would also explain the low levels of H_2S released with L-cys versus **6** and **7**.

Many groups have reported the use of disulfide bridges to covalently cross-link and stabilize the cores of polymeric micelles. The stabilized micelles can be degraded in their cores by disulfide exchange, which would suggest that thiols, such as L-cys and glutathione, have the capacity to infiltrate these often rigid and hydrophobic domains.[69,70] In our case, we envisage a similar capability of L-cys to access thioamides localized in the micelle core. The higher level of H_2S released by polymer **6** versus polymer **7** is most likely due to the greater ability of L-cys to access the corona versus the core. However, this rationalization does not explain the low levels of H_2S released by copolymer **5** with L-cys. One explanation for this observation is that, since hydrolysis is more significant for unimers of **5** (which is evident when L-cys is excluded), a greater proportion of thioamides in solution are consumed via this process, as compared to the micelle-forming polymers **6** and **7**. Therefore, since hydrolysis always occurs in the background in an aqueous environment, less thioamides could be available for activation by L-cys.

To provide further evidence for the ability of the synthesized polymers to function as macromolecular H_2S donors, we carried out a Methylene Blue (MB^+) test, an alternative method for quantitating the amount of H_2S released based on colorimetric detection. However, this methodology suffers from several drawbacks. Dimeric and trimeric forms of MB^+ can coexist with the monomeric form, and these species have different wavelength maxima and molar absorptivity values compared to MB^+, meaning that the absorbance spectra for standard solutions do not always obey Beer's Law. Further, as opposed to the amperometric method (which measures $[H_2S]$ in situ and in real time), the MB^+ method involves sampling of the thioamide stock solution, which necessitates opening the vessel (to the outside air). This may shift the H_2S/HS^- equilibrium and change the $[H_2S]$ in solution. We carried out this test for our polymers in the presence of L-cys, primarily to ensure that the $[H_2S]$ measured using the amperometric method was in a similar concentration range as that measured using the MB^+ test. The peaking concentrations achieved for micellar solutions of thioamide block copolymers **6** and **7**, as measured using the MB^+ method, were found to be in a similar range to those obtained by the amperometric method (Figure S21), although the peaking concentration achieved for block copolymer **6** (187 μM) was found to be slightly lower than that achieved by **7** (211 μM). This small discrepancy is of little concern, given the issues discussed above, which can affect the $[H_2S]$ during the measurement. However, in contrast to **6** and **7**, when we carried out the test for water-soluble polymer **5**, we found that the MB^+ dye discolored within an hour. We investigated literature with regard to this, and it was noted that thiols themselves can be subjected to oxidation to their corresponding disulfide by MB^+, with concurrent reduction of MB^+ to the colorless leucomethylene blue (LMB^+) (Figure S23).[71] The discoloration observed in the case of polymer **5** could indicate that more L-cys was available to reduce MB^+ compared to the block copolymers **6** and **7**, which showed a high level of L-cys-triggered H_2S release in the amperometric studies.

Biological Evaluation of H_2S Donating Polymer 6. *Cell Signaling Tests.* H_2S has the potential to elicit a wide range of physiological actions, including vasodilation and anti-inflammatory effects. The specific molecular targets with which H_2S interacts are thought to include intracellular proteins, enzymes, and transcription factors, as well as membrane ion channels. For example, intracellular H_2S signaling is involved in the endoplasmic reticulum (ER) stress response, where stressed cells turn off protein synthesis to permit the repair of cellular damage. In this case, the generation of H_2S is thought to inhibit a key enzyme, PTP1B, which is localized to the cytoplasmic face of the ER.[72] Ideally, to elicit such a cellular response using a delivery vehicle, the proximity to the target (e.g., the ER) and the timing of H_2S release would be important factors to consider. An ideal carrier would be able to release the requisite amount of H_2S in the cytosol with sufficient spatiotemporal precision to mimic endogenous production.

H_2S release in a cell, whether endogenous or exogenous, can affect signaling pathways that regulate cell behavior. This makes H_2S delivery a potentially powerful strategy for targeting a range of pathological cellular processes. Genetically encoded fluorescent proteins have made it possible to monitor complex signaling events in living cells. Specifically, FRET-based sensors which undergo a conformational change in response to stimuli that activate the kinases, ERK[51] and PKC,[52] have found significant utility in this context. While traditional methods (such as Western blotting or immunostaining) provide a static snapshot of cellular events, FRET-based reporters allow for the dynamic examination of kinase activity with fine spatial and temporal resolution.

Previous studies have reported increases in ERK activity in HEK293 cells in response to H_2S generated as a result of overexpression of cystathionine-γ-lyase.[73] In this work we monitored the effect of macromolecular H_2S-donor **6** on cytosolic and nuclear ERK activity in HEK293 cells using the ERK activity sensor, "EKAR" (extracellular signal regulated kinase activity reporter).[51] ERK activation leads to phosphor-

DOI: 10.1021/acs.biomac.5b01469
Biomacromolecules XXXX, XXX, XXX−XXX

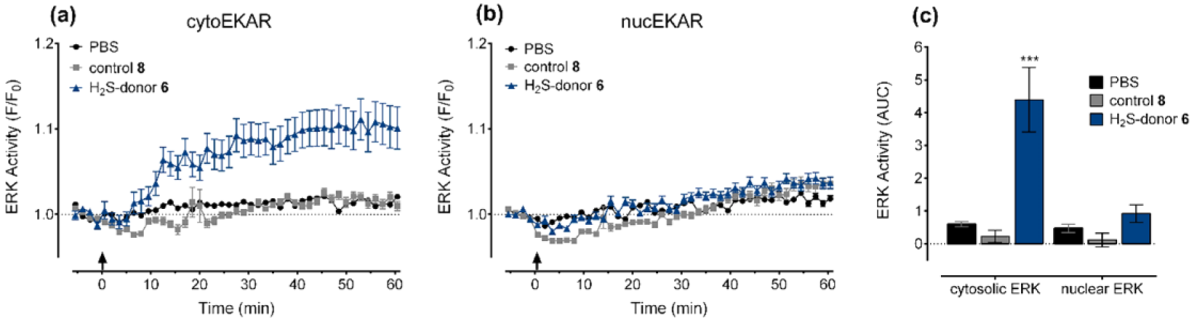

Figure 3. Time course of cytosolic (cyto) ERK activation (a) and nuclear (nuc) ERK activation (b) in HEK293 cells in response to addition of PBS, macromolecular H_2S donor **6** and control **8**, as monitored using EKAR sensor. Area under the curve (AUC) derived from time course (c). Symbols/bars represent means, and error bars SEM of 174−270 cells. ***$p < 0.001$ vs PBS, two-way ANOVA with Dunnett's multiple comparison test.

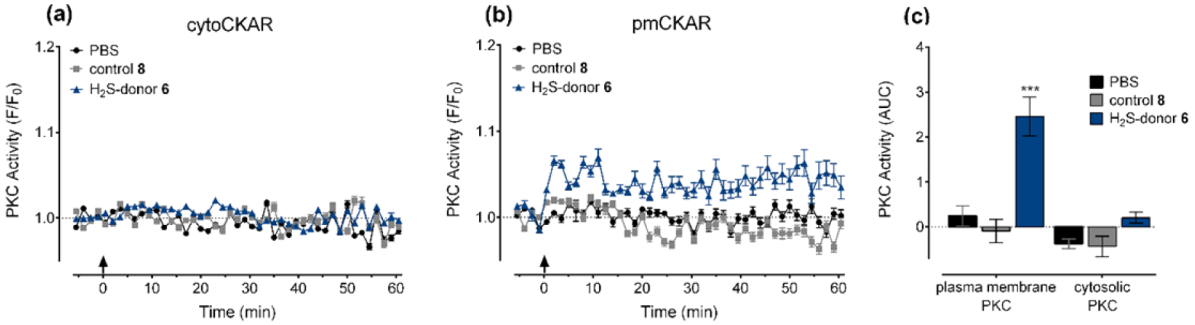

Figure 4. Time course of cytosolic (cyto) PKC activation (a) and plasma membrane-localized (pm) PKC activation (b) in HEK293 cells in response to addition of PBS, H_2S-donating polymer **6** and control polymer **8**, as monitored using CKAR sensor. Area under the curve (AUC) derived from time course (c). Symbols/bars represent means, and error bars SEM of 73−145 cells. ***$p < 0.001$ vs PBS, two-way ANOVA with Dunnett's multiple comparison test.

ylation of EKAR which triggers a conformational change that subsequently increases FRET between donor and acceptor fluorophores in the structure of EKAR. This test was also carried out on a control polymer, [POEGMA$_a$]-*block*-[PMMA$_b$]-H **8** (derived from [POEGMA$_{47}$]-*block*-[PMMA$_{120}$]-S(C═S)Ph), which was synthesized to contain no thioamide moieties (i.e., was unable to release H_2S). Baseline signaling was measured in cells over 6 min, followed by the addition of polymer (either macromolecular control **8** or H_2S donor **6**), and the response was measured over 1 h. A positive control for signaling (used to generate a maximal increase in the signaling pathway) was measured, allowing only cells that responded to the positive control to be selected for analysis. Figure 3 shows the time course data for changes in cytosolic ERK activity over 1 h, expressed as [FRET]/[FRET at time 0] (F/F_0 with each cell normalized to its own baseline FRET level). As can be seen in Figure 3, there was no change in ERK activity in response to the PBS or the control polymer **8**. However, the macromolecular H_2S donor **6** was found to cause a slow and sustained increase in cytosolic ERK from around 5−10 min post-addition (Figure 3a). No effect was seen for any of the materials on ERK activity within the nucleus (Figure 3b). Figure 3c shows the combined area under the curves (AUC) for ERK activity.

The effect of adding macromolecular H_2S-donor **6** on cytosolic and plasma membrane PKC activity in HEK293 cells was also measured using a reporter for PKC-mediated phosphorylation, CKAR (C kinase activity reporter).[52] Previous studies in rat cardiomyocytes demonstrated translocation of PKC to the membrane following addition of the H_2S donor, NaHS.[74] Here, we found that the macromolecular H_2S donor **6** caused a small but fast and sustained increase in plasma membrane (pm)-localized PKC activity immediately following addition to cells (Figure 4b). There was no change in PKC activity in response to PBS or the control **8**. There was also no effect of any of the materials on PKC activity within the cytosol (Figure 4a). Activation of plasma membrane PKC activity for macromolecular H_2S donor **6** is summarized in Figure 4c, which is the combined AUC plot.

Intracellular Live-Cell Imaging. Chemoselective H_2S-responsive fluorescent probes also provide a mechanism by which to image the production of H_2S in live cells with temporal resolution. One example is the use of molecular imaging probes that rely on the selective H_2S-mediated reduction of biocompatible azides to amines for H_2S detection.[75] We applied the probe SF4,[76] which becomes fluorescent in the presence of H_2S (as shown in Figure 5) to image and monitor the release of H_2S in cells over time.

First, the fluorescence generated in HEK293 cells which had been incubated with macromolecular H_2S donor **6** and SF4 probe was monitored over time. Specifically, cells were preincubated with the SF4 probe for 10 min, the baseline fluorescence measured, followed by addition of the macro-

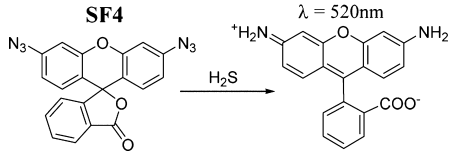

Figure 5. Fluorescent probe SF4 for H_2S detection.

DOI: 10.1021/acs.biomac.5b01469
Biomacromolecules XXXX, XXX, XXX−XXX

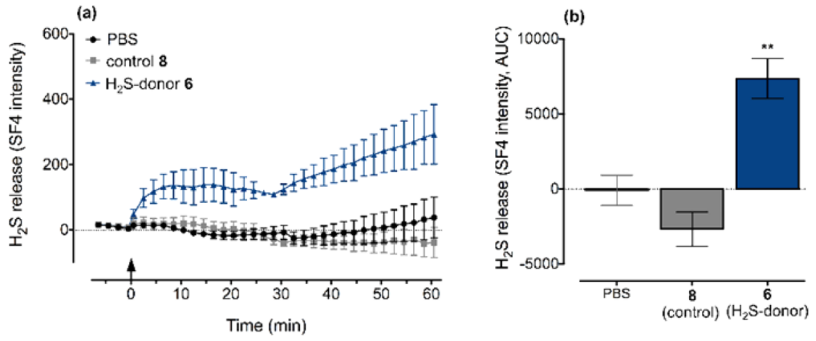

Figure 6. Fluorescence intensity of the SF4 probe over time (a) in HEK293 cells in response to addition of PBS, H_2S-donating polymer **6** and control polymer **8**. Cells loaded with 5 μM SF4 probe in HBSS, polymers loaded at 0.1 mg/mL. Area under the curve (AUC) derived from the time course (b). Symbols/bars represent means, and error bars SEM from three independent experiments conducted in triplicate. $^{**}p < 0.01$ vs PBS, one-way ANOVA with Dunnett's multiple comparison test.

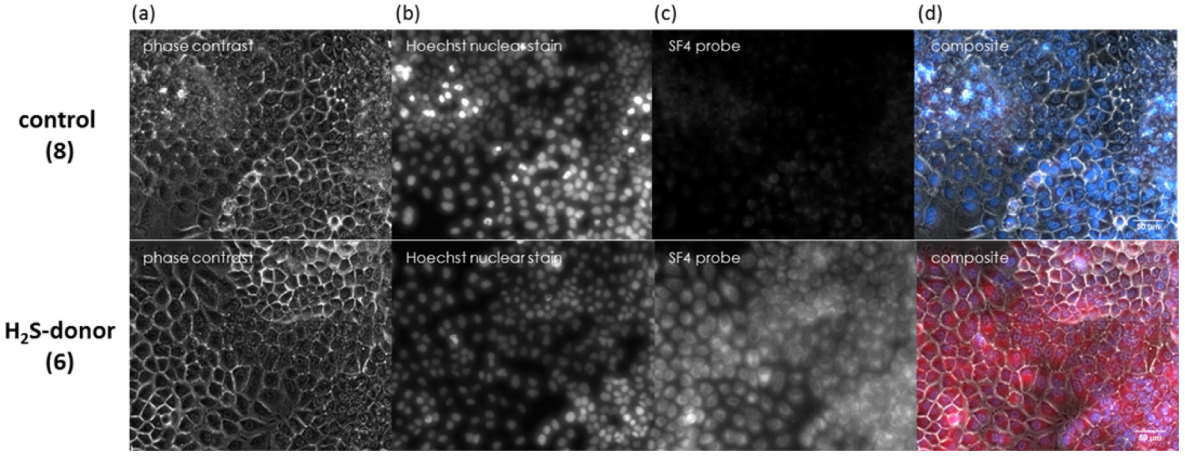

Figure 7. H_2S detection in live H460 lung carcinoma cells using H_2S fluorescent probe SF4. Images in top row show H460 cells incubated for 2 h with control polymer (0.5 mg/mL in OptiMEM), images in bottom row show H460 cells incubated for 2 h with macromolecular H_2S donor **6** (0.5 mg/mL in OptiMEM). Following incubation with polymers, cells were incubated with 5 μM SF4 solution for 30 min and imaged: (a) phase contrast, (b) Hoechst stain, (c) SF4 fluorescence, and (d) composite images showing Hoechst stain in blue and SF4 fluorescence in red.

molecular donor **6**. Fluorescence intensity was measured every 2 min for 1 h, with each measurement carried out in triplicate. As can be seen in Figure 6 (which is the averaged fluorescence result) only addition of the macromolecular H_2S donor **6** increased SF4 fluorescence, corresponding to intracellular release of H_2S. There was no change in SF4 fluorescence following addition of PBS nor the control polymer **8**. Importantly, from these results it can be seen that the release of H_2S from the macromolecular donor correlates with the signaling response measured using the FRET sensors, with both experiments conducted under the same conditions.

To confirm that the macromolecular H_2S donors were effective for H_2S release in multiple cell lines, a further experiment was conducted using H460 lung carcinoma cells. The H460 cells were initially incubated with solutions of either control polymer or macromolecular H_2S donor **6** (2 h), and then treated with Hoechst nuclear stain, followed by SF4 probe (5 μM) for 30 min. As shown in Figure 7, significant intracellular fluorescence was detected with SF4 probe from cells treated with macromolecular H_2S donor **6** (bottom c), relative to cells treated with the control polymer (top c). Moreover, bright-field images with Hoechst nuclear staining confirmed that the cells remain viable throughout exposure to the donor (b).

CONCLUSION

In conclusion, a series of benzonitrile-functionalized polymers were synthesized and successfully transformed into primary aryl thioamide-functionalized polymers using a postpolymerization approach. The use of RAFT polymerization enabled incorporation of the thioamides into a hydrophilic polymer or into either the hydrophilic or the hydrophobic domain of a block copolymer. The block copolymers were designed to form micelles in PBS, while the hydrophilic, water-soluble copolymer afforded unimers. We demonstrated that these thioamide-functionalized polymers were effective as macromolecular H_2S donors and that release of H_2S occurred either hydrolytically or in response to a thiol stimulus. Specifically, L-cysteine-triggered H_2S release was significant for micelles of the macromolecular H_2S donor, resulting in release of more than 3× as much H_2S from the thioamide units, compared to the water-soluble polymer. Incorporation of the thioamides into the corona versus the core further enhanced the process. The hydrolysis mechanism results in lower, yet sustained release over time and proved to be most significant for water-soluble polymer.

The macromolecular H_2S donors synthesized with the thioamide moieties in the hydrophilic domains were subsequently applied in a range of cellular tests. The macromolecular H_2S donors were found to elicit a slow and sustained increase in cytosolic ERK signaling in HEK293 cells, as

DOI: 10.1021/acs.biomac.5b01469
Biomacromolecules XXXX, XXX, XXX−XXX

monitored using a FRET-based ERK activity sensor. The donors were also found to cause a small, fast, and sustained increase in plasma membrane-localized PKC activity immediately following addition to cells. Finally, an H_2S-selective probe that becomes fluorescent on reaction with H_2S enabled further confirmation of the release of H_2S from the polymer inside live cells. The macromolecular H_2S donors caused an increase in fluorescence over time, which correlates with the time frame of signaling responses, as measured using the FRET reporters. Taken together, these results demonstrate that macromolecular H_2S donors are capable of stimulating spatiotemporally confined changes to cell signaling. Moreover, we postulate that, with further modification of the chemical structure of the macromolecular donor, it may become possible to target particular signaling processes in an increasingly refined manner.

■ ASSOCIATED CONTENT

Supporting Information

The Supporting Information is available free of charge on the ACS Publications website at DOI: 10.1021/acs.biomac.5b01469.

Full synthetic details of all polymers and small molecules; characterization data (^{1}H NMR spectra, GPC traces, ATR-FTIR and DLS); considerations and equations for H_2S kinetics; experimental methods for cell work (PDF).

■ AUTHOR INFORMATION

Corresponding Authors

*E-mail: thomas.p.davis@monash.edu.
*E-mail: michelle.halls@monash.edu.
*E-mail: john.f.quinn@monash.edu.

Notes

The authors declare no competing financial interest.

■ ACKNOWLEDGMENTS

This work was carried out within the Australian Research Council (ARC) Centre of Excellence in Convergent Bio-Nano Science and Technology (Project No. CE140100036). T.P.D. is grateful for the award of an Australian Laureate Fellowship from the ARC and M.K. for the award of an NHMRC Senior Research Fellowship. M.L.H. is supported by a National Health and Medical Research Council of Australia (NHMRC) RD Wright Fellowship (1061687). T.P.D., M.R.W., and J.F.Q. acknowledge financial support from the Faculty of Pharmacy and Pharmaceutical Sciences, Monash University and from the Monash-Warwick Alliance.

■ REFERENCES

(1) Abe, K.; Kimura, H. The possible role of hydrogen sulfide as an endogenous neuromodulator. *J. Neurosci.* **1996**, *16*, 1066−1071.

(2) Wang, R. Physiological Implications of Hydrogen Sulfide: A Whiff Exploration That Blossomed. *Physiol. Rev.* **2012**, *92*, 791−896.

(3) Olson, K. R. The therapeutic potential of hydrogen sulfide: separating hype from hope. *Am. J. Physiol.: Regul., Integr. Comp. Physiol.* **2011**, *301*, R297−R312.

(4) Fukuto, J. M.; Carrington, S. J.; Tantillo, D. J.; Harrison, J. G.; Ignarro, L. J.; Freeman, B. A.; Chen, A.; Wink, D. A. Small Molecule Signaling Agents: The Integrated Chemistry and Biochemistry of Nitrogen Oxides, Oxides of Carbon, Dioxygen, Hydrogen Sulfide, and Their Derived Species. *Chem. Res. Toxicol.* **2012**, *25*, 769−793.

(5) Li, L.; Rose, P.; Moore, P. K. Hydrogen Sulfide and Cell Signaling. *Annu. Rev. Pharmacol. Toxicol.* **2011**, *51*, 169−187.

(6) Martelli, A.; Testai, L.; Breschi, M. C.; Blandizzi, C.; Virdis, A.; Taddei, S.; Calderone, V. Hydrogen sulphide: novel opportunity for drug discovery. *Med. Res. Rev.* **2012**, *32*, 1093−1130.

(7) Hildebrandt, T. M.; Grieshaber, M. K. Three enzymatic activities catalyze the oxidation of sulfide to thiosulfate in mammalian and invertebrate mitochondria. *FEBS J.* **2008**, *275*, 3352−3361.

(8) Chen, X. L.; Jhee, K. H.; Kruger, W. D. Production of the neuromodulator H_2S by cystathionine beta-synthase via the condensation of cysteine and homocyste ine. *J. Biol. Chem.* **2004**, *279*, 52082−52086.

(9) Mikami, Y.; Shibuya, N.; Ogasawara, Y.; Kimura, H. Hydrogen sulfide is produced by cystathionine gamma-lyase at the steady-state low intracellular Ca^{2+} concentrations. *Biochem. Biophys. Res. Commun.* **2013**, *431*, 131−135.

(10) Muenchberg, U.; Anwar, A.; Mecklenburg, S.; Jacob, C. Polysulfides as biologically active ingredients of garlic. *Org. Biomol. Chem.* **2007**, *5*, 1505−1518.

(11) Mustafa, A. K.; Sikka, G.; Gazi, S. K.; Steppan, J.; Jung, S. M.; Bhunia, A. K.; Barodka, V. M.; Gazi, F. K.; Barrow, R. K.; Wang, R.; Amzel, L. M.; Berkowitz, D. E.; Snyder, S. H. Hydrogen Sulfide as Endothelium-Derived Hyperpolarizing Factor Sulfhydrates Potassium Channels. *Circ. Res.* **2011**, *109*, 1259−U1169.

(12) Zhao, W. M.; Zhang, J.; Lu, Y. J.; Wang, R. The vasorelaxant effect of H_2S as a novel endogenous gaseous K-ATP channel opener. *EMBO J.* **2001**, *20*, 6008−6016.

(13) Gemici, B.; Wallace, J. L. Anti-inflammatory and cytoprotective properties of hydrogen sulfide. *Methods Enzymol.* **2015**, *555*, 169−193.

(14) Zanardo, R. C. O.; Brancaleone, V.; Distrutti, E.; Fiorucci, S.; Cirino, G.; Wallace, J. L. Hydrogen sulfide is an endogenous modulator of leukocyte-mediated inflammation. *FASEB J.* **2006**, *20*, E1411−E4118.

(15) Lefer, D. J. A new gaseous signaling molecule emerges: Cardioprotective role of hydrogen sulfide. *Proc. Natl. Acad. Sci. U. S. A.* **2007**, *104*, 17907−17908.

(16) Wang, X.; Wang, Q.; Guo, W.; Zhu, Y. Z. Hydrogen sulfide attenuates cardiac dysfunction in a rat model of heart failure: a mechanism through cardiac mitochondrial protection. *Biosci. Rep.* **2011**, *31*, 87−98.

(17) Yang, G.; Wu, L.; Jiang, B.; Yang, W.; Qi, J.; Cao, K.; Meng, Q.; Mustafa, A. K.; Mu, W.; Zhang, S.; Snyder, S. H.; Wang, R. H_2S as a physiologic vasorelaxant: Hypertension in mice with deletion of cystathionine gamma-lyase. *Science* **2008**, *322*, 587−590.

(18) Kimura, H.; Nagai, Y.; Umemura, K.; Kimura, Y. Physiological roles of hydrogen sulfide: Synaptic modulation, neuroprotection, and smooth muscle relaxation. *Antioxid. Redox Signaling* **2005**, *7*, 795−803.

(19) Lee, M.; Schwab, C.; Yu, S.; McGeer, E.; McGeer, P. L. Astrocytes produce the antiinflammatory and neuroprotective agent hydrogen sulfide. *Neurobiol. Aging* **2009**, *30*, 1523−1534.

(20) Hu, L.-F.; Lu, M.; Tiong, C. X.; Dawe, G. S.; Hu, G.; Bian, J.-S. Neuroprotective effects of hydrogen sulfide on Parkinson's disease rat models. *Aging Cell* **2010**, *9*, 135−146.

(21) Medeiros, J. V. R.; Bezerra, V. H.; Gomes, A. S.; Barbosa, A. L. R.; Lima-Junior, R. C. P.; Soares, P. M. G.; Brito, G. A. C.; Ribeiro, R. A.; Cunha, F. Q.; Souza, M. H. L. P. Hydrogen Sulfide Prevents Ethanol-Induced Gastric Damage in Mice: Role of ATP-Sensitive Potassium Channels and Capsaicin-Sensitive Primary Afferent Neurons. *J. Pharmacol. Exp. Ther.* **2009**, *330*, 764−770.

(22) Wu, L.; Yang, W.; Jia, X.; Yang, G.; Duridanova, D.; Cao, K.; Wang, R. Pancreatic islet overproduction of H_2S and suppressed insulin release in Zucker diabetic rats. *Lab. Invest.* **2009**, *89*, 59−67.

(23) Wallace, J. L.; Dicay, M.; McKnight, W.; Martin, G. R. Hydrogen sulfide enhances ulcer healing in rats. *FASEB J.* **2007**, *21*, 4070−4076.

(24) Predmore, B. L.; Lefer, D. J.; Gojon, G. Hydrogen Sulfide in Biochemistry and Medicine. *Antioxid. Redox Signaling* **2012**, *17*, 119−140.

(25) Du, J. B.; Hui, Y.; Cheung, Y. F.; Bin, G.; Jiang, H. F.; Chen, X. B.; Tang, C. S. The possible role of hydrogen sulfide as a smooth

DOI: 10.1021/acs.biomac.5b01469
Biomacromolecules XXXX, XXX, XXX−XXX

muscle cell proliferation inhibitor in rat cultured cells. *Heart Vessels* **2004**, *19*, 75−80.
(26) Papapetropoulos, A.; Pyriochou, A.; Altaany, Z.; Yang, G.; Marazioti, A.; Zhou, Z.; Jeschke, M. G.; Branski, L. K.; Herndon, D. N.; Wang, R.; Szabo, C. Hydrogen sulfide is an endogenous stimulator of angiogenesis. *Proc. Natl. Acad. Sci. U. S. A.* **2009**, *106*, 21972−21977.
(27) Osipov, R. M.; Robich, M. P.; Feng, J.; Chan, V.; Clements, R. T.; Deyo, R. J.; Szabo, C.; Sellke, F. W. Effect of hydrogen sulfide on myocardial protection in the setting of cardioplegia and cardiopulmonary bypass. *Interact. Cardiovasc. Thorac. Surg.* **2010**, *10*, 506−512.
(28) Rinaldi, L.; Gobbi, G.; Pambianco, M.; Micheloni, C.; Mirandola, P.; Vitale, M. Hydrogen sulfide prevents apoptosis of human PMN via inhibition of p38 and caspase 3. *Lab. Invest.* **2006**, *86*, 391−397.
(29) Hu, L.-F.; Wong, P. T. H.; Moore, P. K.; Bian, J.-S. Hydrogen sulfide attenuates lipopolysaccharide-induced inflammation by inhibition of p38 mitogen-activated protein kinase in microglia. *J. Neurochem.* **2007**, *100*, 1121−1128.
(30) Gobbi, G.; Ricci, F.; Malinverno, C.; Carubbi, C.; Pambianco, M.; de Panfilis, G.; Vitale, M.; Mirandola, P. Hydrogen sulfide impairs keratinocyte cell growth and adhesion inhibiting mitogen-activated protein kinase signaling. *Lab. Invest.* **2009**, *89*, 994−1006.
(31) DeLeon, E. R.; Stoy, G. F.; Olson, K. R. Passive loss of hydrogen sulfide in biological experiments. *Anal. Biochem.* **2012**, *421*, 203−207.
(32) Caliendo, G.; Cirino, G.; Santagada, V.; Wallace, J. L. Synthesis and Biological Effects of Hydrogen Sulfide (H_2S): Development of H_2S-Releasing Drugs as Pharmaceuticals. *J. Med. Chem.* **2010**, *53*, 6275−6286.
(33) Gu, X.; Zhu, Y. Z. Therapeutic applications of organosulfur compounds as novel hydrogen sulfide donors and/or mediators. *Expert Rev. Clin. Pharmacol.* **2011**, *4*, 123−133.
(34) Sparatore, A.; Santus, G.; Giustarini, D.; Rossi, R.; Del Soldato, P. Therapeutic potential of new hydrogen sulfide-releasing hybrids. *Expert Rev. Clin. Pharmacol.* **2011**, *4*, 109−121.
(35) Wallace, J. L. Hydrogen sulfide-releasing anti-inflammatory drugs. *Trends Pharmacol. Sci.* **2007**, *28*, 501−505.
(36) Hasegawa, U.; Van Der Vlies, A. J. Design and Synthesis of Polymeric Hydrogen Sulfide Donors. *Bioconjugate Chem.* **2014**, *25*, 1290−1300.
(37) Hasegawa, U.; Van Der Vlies, A. J. Polymeric micelles for hydrogen sulfide delivery. *MedChemComm* **2015**, *6*, 273−276.
(38) Terwogt, J. M. M.; Huinink, W. W. T.; Schellens, J. H. M.; Schot, M.; Mandjes, I. A. M.; Zurlo, M. G.; Rocchetti, M.; Rosing, H.; Koopman, F. J.; Beijnen, J. H. Phase I clinical and pharmacokinetic study of PNU166945, a novel water-soluble polymer-conjugated prodrug of paclitaxel. *Anti-Cancer Drugs* **2001**, *12*, 315−323.
(39) Vasey, P. A.; Kaye, S. B.; Morrison, R.; Twelves, C.; Wilson, P.; Duncan, R.; Thomson, A. H.; Murray, L. S.; Hilditch, T. E.; Murray, T.; Burtles, S.; Fraier, D.; Frigerio, E.; Cassidy, J. Canc Res Campaign Phase, I. I. I. C. Phase I clinical and pharmacokinetic study of PK1 *N*-(2-hydroxypropyl)methacrylamide copolymer doxorubicin: First member of a new class of chemotherapeutic agents - Drug-polymer conjugates. *Clin. Cancer Res.* **1999**, *5*, 83−94.
(40) Yurkovetskiy, A. V.; Fram, R. J. XMT-1001, a novel polymeric camptothecin pro-drug in clinical development for patients with advanced cancer. *Adv. Drug Delivery Rev.* **2009**, *61*, 1193−1202.
(41) Zhao, Y.; Bhushan, S.; Yang, C.; Otsuka, H.; Stein, J. D.; Pacheco, A.; Peng, B.; Devarie-Baez, N. O.; Aguilar, H. C.; Lefer, D. J.; Xian, M. Controllable Hydrogen Sulfide Donors and Their Activity against Myocardial Ischemia-Reperfusion Injury. *ACS Chem. Biol.* **2013**, *8*, 1283−1290.
(42) Zhao, Y.; Wang, H.; Xian, M. Cysteine-Activated Hydrogen Sulfide (H_2S) Donors. *J. Am. Chem. Soc.* **2011**, *133*, 15−17.
(43) Martelli, A.; Testai, L.; Citi, V.; Marino, A.; Pugliesi, I.; Barresi, E.; Nesi, G.; Rapposelli, S.; Taliani, S.; Da Settimo, F.; Breschi, M. C.; Calderone, V. Arylthioamides as H_2S Donors: L-Cysteine-Activated Releasing Properties and Vascular Effects in Vitro and in Vivo. *ACS Med. Chem. Lett.* **2013**, *4*, 904−908.
(44) Zhao, Y.; Kang, J.; Park, C.-M.; Bagdon, P. E.; Peng, B.; Xian, M. Thiol-Activated gem-Dithiols: A New Class of Controllable Hydrogen Sulfide Donors. *Org. Lett.* **2014**, *16*, 4536−4539.
(45) Foster, J. C.; Powell, C. R.; Radzinski, S. C.; Matson, J. B. S-Aroylthiooximes: A Facile Route to Hydrogen Sulfide Releasing Compounds with Structure-Dependent Release Kinetics. *Org. Lett.* **2014**, *16*, 1558−1561.
(46) Roger, T.; Raynaud, F.; Bouillaud, F.; Ransy, C.; Simonet, S.; Crespo, C.; Bourguignon, M.-P.; Villeneuve, N.; Vilaine, J.-P.; Artaud, I.; Galardon, E. New biologically active hydrogen sulfide donors. *ChemBioChem* **2013**, *14*, 2268−2271.
(47) Foster, J. C.; Matson, J. B. Functionalization of Methacrylate Polymers with Thiooximes: A Robust Postpolymerization Modification Reaction and a Method for the Preparation of H2S-Releasing Polymers. *Macromolecules* **2014**, *47*, 5089−5095.
(48) Antibe Therapeutics Inc. Wallace J. L.; Cirino G.; Santagada V.; Caliendo G. Hydrogen sulfide derivatives of nonsteroidal anti-inflammatory drugs. U.S. Patent WO/2008/009127, 2008.
(49) Long, T. R.; Wongrakpanich, A.; Do, A.-V.; Salem, A. K.; Bowden, N. B. *Polym. Chem.* **2015**, *6*, 7188−7195.
(50) Verzijl, D.; Storelli, S.; Scholten, D. J.; Bosch, L.; Reinhart, T. A.; Streblow, D. N.; Tensen, C. P.; Fitzsimons, C. P.; Zaman, G. J. R.; Pease, J. E.; de Esch, I. J. P.; Smit, M. J.; Leurs, R. *J. Pharmacol. Exp. Ther.* **2008**, *325*, 544−555.
(51) Harvey, C. D.; Ehrhardt, A. G.; Cellurale, C.; Zhong, H.; Yasuda, R.; Davis, R. J.; Svoboda, K. A genetically encoded fluorescent sensor of ERK activity. *Proc. Natl. Acad. Sci. U. S. A.* **2008**, *105*, 19264−19269.
(52) Violin, J. D.; Zhang, J.; Tsien, R. Y.; Newton, A. C. A genetically encoded fluorescent reporter reveals oscillatory phosphorylation by protein kinase C. *J. Cell Biol.* **2003**, *161*, 899−909.
(53) Gallegos, L. L.; Kunkel, M. T.; Newton, A. C. Targeting protein kinase C activity reporter to discrete intracellular regions reveals spatiotemporal differences in agonist-dependent signaling. *J. Biol. Chem.* **2006**, *281*, 30947−30956.
(54) Halls, M. L.; Poole, D. P.; Ellisdon, A. M.; Nowell, C. J.; Canals, M. Detection and Quantification of Intracellular Signaling Using FRET-Based Biosensors and High Content Imaging. *Methods Mol. Biol. (N. Y., NY, U. S.)* **2015**, *1335*, 131−161.
(55) Schindelin, J.; Arganda-Carreras, I.; Frise, E.; Kaynig, V.; Longair, M.; Pietzsch, T.; Preibisch, S.; Rueden, C.; Saalfeld, S.; Schmid, B.; Tinevez, J.-Y.; White, D. J.; Hartenstein, V.; Eliceiri, K.; Tomancak, P.; Cardona, A. Fiji: an open-source platform for biological-image analysis. *Nat. Methods* **2012**, *9*, 676−682.
(56) Jagodzinski, T. S. Thioamides as useful synthons in the synthesis of heterocycles. *Chem. Rev.* **2003**, *103*, 197−227.
(57) Crank, G.; Mursyidi, A. Photochemical - Reactions of Thioamides. *J. Photochem. Photobiol., A* **1990**, *53*, 301−310.
(58) Lackner, A. M.; Margerum, J. D.; Sherman, E.; Coates, D. Liquid crystal monomer additives for improved polymer dispersed liquid crystals. *Mol. Cryst. Liq. Cryst. Sci. Technol., Sect. A* **1995**, *261*, 593−603.
(59) Manaka, A.; Sato, M. Synthesis of aromatic thioamide from nitrile without handling of gaseous hydrogen sulfide. *Synth. Commun.* **2005**, *35*, 761−764.
(60) Kabachii, Y. A.; Kochev, S. Y. Alcoholysis and aminolysis of Di- and trithioester chain-transfer agents of free-radical polymerization. *Polym. Sci., Ser. A* **2006**, *48*, 717−722.
(61) Chong, Y. K.; Moad, G.; Rizzardo, E.; Thang, S. H. Thiocarbonylthio end group removal from RAFT-synthesized polymers by radical-induced reduction. *Macromolecules* **2007**, *40*, 4446−4455.
(62) Crane, L. J.; Anastassiadou, M.; Stigliani, J. L.; Baziard-Mouysset, G.; Payard, M. Reactions of some ortho and para halogenated aromatic nitriles with ethylenediamine: selective synthesis of imidazolines. *Tetrahedron* **2004**, *60*, 5325−5330.
(63) Walter, W.; Voss, J. The chemistry of thioamides. In *Amides*; Zabicky, J., Ed.; John Wiley & Sons, Ltd: Chichester, U.K., 1970; Chapter 8, pp 385−464.

DOI: 10.1021/acs.biomac.5b01469
Biomacromolecules XXXX, XXX, XXX−XXX

(64) Jeroschewski, P.; Steuckart, C.; Kuhl, M. An amperometric microsensor for the determination of H_2S in aquatic environments. *Anal. Chem.* **1996**, *68*, 4351−4357.
(65) Broderius, S. J.; Smith, L. L. Direct Determination and Calculation of Aqueous Hydrogen-Sulfide. *Anal. Chem.* **1977**, *49*, 424−428.
(66) Rosenthal, D.; Taylor, T. I. A Study of the Mechanism and Kinetics of the Thioacetamide Hydrolysis Reaction. *J. Am. Chem. Soc.* **1957**, *79*, 2684−2690.
(67) Hall, A. J.; Satchell, D. P. Acylation 38. Kinetics and Mechanism of Hydrogen Ion Catalyzed-Hydrolysis of Thiobenzamide. *J. Chem. Soc., Perkin Trans. 2* **1974**, 1077−1080.
(68) Schlatter, M. J. The reaction between thioamides and primary amines. *J. Am. Chem. Soc.* **1942**, *64*, 2722−2722.
(69) Ryu, J.-H.; Roy, R.; Ventura, J.; Thayumanavan, S. Redox-Sensitive Disassembly of Amphiphilic Copolymer Based Micelles. *Langmuir* **2010**, *26*, 7086−7092.
(70) Koo, A. N.; Lee, H. J.; Kim, S. E.; Chang, J. H.; Park, C.; Kim, C.; Park, J. H.; Lee, S. C. Disulfide-cross-linked PEG-poly(amino acid)s copolymer micelles for glutathione-mediated intracellular drug delivery. *Chem. Commun.* **2008**, 6570−6572.
(71) Earl S. H.; Hsiao-Nein, T. In Organic Free Radicals. *ACS Symposium Series*; ACS: Washington, DC, 1978; Vol. *69*, Ch 15, pp 258−274.
(72) Krishnan, N.; Fu, C.; Pappin, D. J.; Tonks, N. K. H_2S-Induced Sulfhydration of the Phosphatase PTP1B and Its Role in the Endoplasmic Reticulum Stress Response. *Sci. Signaling* **2011**, *4* (203), ra86.
(73) Yang, G. D.; Cao, K.; Wu, L. Y.; Wang, R. Cystathionine gamma-lyase overexpression inhibits cell proliferation via a H_2S-dependent modulation of ERK1/2 phosphorylation and p21(Cip/WAK-1). *J. Biol. Chem.* **2004**, *279*, 49199−49205.
(74) Pan, T.-T.; Neo, K. L.; Hu, L.-F.; Yong, Q. C.; Bian, J.-S. H_2S preconditioning-induced PKC activation regulates intracellular calcium handling in rat cardiomyocytes. *Am. J. Physiol.: Cell Physiol.* **2008**, *294*, C169−C177.
(75) Sasmal, P. K.; Carregal-Romero, S.; Han, A. A.; Streu, C. N.; Lin, Z.; Namikawa, K.; Elliott, S. L.; Koester, R. W.; Parak, W. J.; Meggers, E. Catalytic Azide Reduction in Biological Environments. *ChemBioChem* **2012**, *13*, 1116−1120.
(76) Lin, V. S.; Lippert, A. R.; Chang, C. J. Cell-trappable fluorescent probes for endogenous hydrogen sulfide signaling and imaging H_2O_2-dependent H_2S production. *Proc. Natl. Acad. Sci. U. S. A.* **2013**, *110*, 7131−7135.

DOI: 10.1021/acs.biomac.5b01469
Biomacromolecules XXXX, XXX, XXX−XXX